water

MDPI

Article

Ultraviolet Radiation-Assisted Preparation of a Novel Biomass Fiber to Remove Cadmium from Wastewater

Hao Xue [1], Min Xu [1], Yueyang Yu [2], Jiancheng Wan [3], Chen Liu [3,*] and Fansheng Meng [1,*]

[1] Chinese Research Academy of Environmental Sciences, Beijing 100012, China
[2] Qiantang River Basin Management Center of Zhejiang Province, Hangzhou 310016, China
[3] Hangzhou Shenyuan Environmental Sci-Tech Co., Ltd., Hangzhou 310016, China
* Correspondence: lcah119@163.com (C.L.); mengfs@craes.org.cn (F.M.)

Abstract: The heavy metal adsorbents developed based on biomass resources have valuable application prospects due to the characteristics of rich sources, renewability and low cost. In the present work, a carboxyl functioned loofah fiber (LF@AA) was synthesized via UV-induced polymerization, and its adsorption capacity for cadmium (Cd^{2+}) was investigated systematically. This modification resulted in the effective combination of a loofah fiber template and polyacrylic acid (PAA), which promoted its adsorption of Cd^{2+} to significantly increase to 339.3 mg·g^{-1}, and the applicable pH range was 4.0~7.0. Furthermore, the adsorbability of LF@AA remained stable at a high level after eight consecutive cycles. The adsorption kinetics and isotherm parameters revealed that the adsorption characteristics of cadmium conformed to the Weber–Morris and pseudo-second-order kinetics equations, and the adsorption process of cadmium conformed to Redlich–Peterson and Langmuir models. In addition, consequences of EDS, FTIR, and Zeta potential analysis reflected that the main adsorption mechanism should be ion exchange. Cd^{2+} was drawn to the adsorbent surface by electrostatic binding, and ion exchange occurred to form a bidentate chelate. This study suggests that it is reasonable and feasible to use natural biomass materials to develop efficient adsorbents to treat heavy metal pollution in wastewater.

Keywords: adsorption; Cd^{2+}; biomass fiber; modification; kinetics

check for updates

Citation: Xue, H.; Xu, M.; Yu, Y.; Wan, J.; Liu, C.; Meng, F. Ultraviolet Radiation-Assisted Preparation of a Novel Biomass Fiber to Remove Cadmium from Wastewater. *Water* **2023**, *15*, 811. https://doi.org/10.3390/w15040811

Academic Editor: Alessandro Erto

Received: 2 January 2023
Revised: 15 February 2023
Accepted: 17 February 2023
Published: 19 February 2023

1. Introduction

With the rapid development of industry, the discharge of industrial wastewater containing high-density heavy metals has caused serious water pollution. Cadmium is extensively used in the field of alloy manufacturing, plastic stabilizer manufacturing, pigments and batteries; however, cadmium is very highly toxic, and causes grave harm to living organisms, because it is easily enriched in the vital organs of organisms and has potential carcinogenicity. The European Union treats cadmium as a high-risk carcinogen and toxic agent. The Environmental Protection Agency (EPA) had set its maximum concentrations in drinking water at 10 μg/L and planned to prune it down to 5 μg/L [1]. Therefore, it is meaningful to consider the removal of cadmium from wastewater. Various purification methods have been proposed for the treatment of heavy metals, e.g., chemistry precipitation, reverse osmosis, electrochemical treatment, and so forth [2]. Aside from these, adsorption is highly recommended because it is clean, requires low investment, highly efficient, and easy to operate [3].

Recently, there is a growing interest in the utilization of agricultural by-products or agricultural and forest product processing wastes, such as sugarcane bagasse, pineapple peel, fruit peel, straw, seed shells, and rice husks, to exploit cost-effective adsorbents for the separation and enrichment of heavy metal [4–7]. It is known that a biomass resource has splendid material sources, it is renewable, is low cost, and has particular properties, such as biodegradability, biocompatibility and homogeneity. However, most of these adsorbents do not have superlative performance in adsorption and/or reuse. Many studies on adsorbent

modification methods have recently been carried out, such as heat treatment [8,9], acid treatments, grafting [10], metal oxide loading, and organic compound coating [11]. Among them, UV-induced polymerization is considered to have excellent efficacy because the grafted polymer contains abundant functional groups, resulting in the muscular coordination ability for metal ions [12]. This modification can form a uniform micro-villous layer on the surface without damaging the original structure of the substrate. Specifically, benefitting from properties of the elastic design, convenient control, and tight binding, the UV-induced polymerization not only can realize efficient adsorbent capacity but also keep the excellent properties of the selected substrate [13]. It has been reported that excellent adsorbents have been prepared based on natural minerals and natural polymers (e.g., attapulgite, diatomite, biomass fiber, and silica fume) by UV-induced polymerization [12–15].

Loofah sponge fiber (LF), which is the vascular bundle of the dried ripe fruit of *Luffa cylindrica* (L.) *Roem* is known for its complex interconnecting porous structure, which has conspicuous mechanical properties and practical surface chemistry characteristics at remarkably low densities [16–18]. Furthermore, LF is often used as a natural adsorbent due to its numerous advantages, including effectiveness, being innoxious, cost-effectiveness, multi-hole properties, ruggedness, and biodegradability [19,20]. At present, due to its microsponge structure and large number of micro-cell fibers, natural LF can be nominated as a great candidate for the separation of pollutants from aqueous solutions in the field of environmental protection. Researchers have used natural LF as an adsorbent or carrier to remove heavy metals, COD, and nitrogen from wastewater and have achieved good treatment results [21–24].

Natural LF is mainly composed of cellulose/hemicellulose, hemicellulose, lignin, extractives, and ashes, which do not include functional groups of adsorption, as well as ion exchange. However, the LF is rich in hydroxyl groups, which are easily modified by amino groups or carboxylate groups. Several strategies have been suggested to improve the adsorption capacity of natural LF, such as ultraviolet radiation grafts [15,25], microbionation [26,27], composite materials [28–30], activated carbon [31], and modified biochar [32]. However, the literature on the removal of cadmium by these agricultural by-products-based adsorbents is still scarce, and to the best of our knowledge, the adsorbent functionalized loofah sponge structure with carboxyl groups (LF@AA) for the recovery of cadmium has not been reported.

This paper aims to prepare LF@AA supported on LF's three-dimensional natural polymer networks via UV-induced polymerization and verify its removal ability of Cd^{2+} from wastewater. The physical and chemical characterization of LF@AA was conducted. Several batches of adsorption experiments were carried out to study the effects of pH, ionic strength, cycle number, kinetics, and isotherms on adsorption. The regeneration of the materials was also studied for potential practical applications. Through this study, the mechanisms for Cd^{2+} removal were better understood.

2. Materials and Methods

2.1. Materials

The LF was obtained from Hubei Province, southern China. Sodium hydroxide (NaOH), acrylic acid (AA), ethanol, acetone, benzophenone (BP), hydrochloric acid (HCl), ferrous ammonium sulfate ($(NH_4)_2Fe(SO_4)_2 \cdot 6H_2O$), and cadmium nitrate ($Cd(NO_3)_2$) were of analytical grade and used as received.

2.2. Synthesis of LF@AA

Typically, the LF washed with ethanol and distilled water was dried at 105 °C for 12 h, and then, particles of 0.05–0.2 cm were screened. The LF&BP was prepared by immersing a certain quality of LF in a certain concentration of BP ethanol solution and drying it at 323.15 K in a vacuum environment. The grafting solution was produced by dissolving a certain amount of AA and ferrous ammonium sulfate into a 25% ethanol solution. The LF&BP soaked (24 h) in the grafting solution was irradiated with ultraviolet light (25 min)

and then washed clean with boiling water to obtain the clean product (LF@AA). LF@AA was then soxhlet extracted (24 h) with acetone, soaked (30 min) in 2.0% NaOH solution, washed, and dried (8 h) in a vacuum at 80 °C. The graft ratio (%) was calculated as follows:

$$\text{Grafting yield } = (W_2 - W_1) \times 100/W_1 \quad (1)$$

where W_1 (g) and W_2 (g) represent the original weight and the grafted weight of the sample, respectively.

2.3. Characterization Analysis

The microscopic characteristics of the samples were respected by scanning electron microscopy (SEM, SU8010, Hitachi, Ltd., Tokyo, Japan) with an energy-dispersive X-ray spectroscopy (XPS, MULT1LAB2000, Thermo Fisher Scientific Inc., Waltham, MA, USA). The spectral changes of samples at different stages were observed via Fourier transform infrared spectrometry (FTIR, Nicolet iS50, Thermo Fisher Scientific Inc., Waltham, MA, USA), the spectra were implemented based on ATR (Attenuated Total Reflection), and the recording range was 4000 to 400 cm^{-1}.

2.4. Factors Affecting Adsorption Properties

The effects of the Cd^{2+} concentration, pH value, interfering ions, and temperature on the adsorption performance of LF@AA were evaluated through adsorption experiments. The Cd^{2+} solution was prepared by dissolving $Cd(NO_3)_2$ salt into deionized water.

Typically, the LF@AA (1.0 $g \cdot L^{-1}$) was added to a certain concentration of the Cd^{2+} solution and stirred for 4 h (150 rpm, 25 °C). After filtration, the concentration of Cd^{2+} in the supernatant was monitored with an inductively coupled plasma emission spectrometer (ICP-8100, Shimadzu Co., Ltd., Kyoto, Japan). The sorption capacity was calculated (Equation (2)).

$$q_e = (C_0 - C_e) \times V/m \quad (2)$$

where q_e is the saturated adsorption capacity ($mg \cdot g^{-1}$), C_0 is the initial concentration of Cd^{2+} ($mg \cdot L^{-1}$), C_e is the equilibrium concentration of Cd^{2+} ($mg \cdot L^{-1}$), V is the volume of Cd^{2+} solutions, and m is the mass of the sorbent (g).

The pH of the solution was adjusted to a range of 2.0–7.0 with 1 M NaOH or HCl. The effect of interfering ions on Cd^{2+} adsorption was determined by adding the adsorbent to Erlenmeyer flasks filled with Cd^{2+} solution (400 $mg \cdot L^{-1}$) and interfering ions (K+, Na^+) of different concentrations from 0 to 100 $mmol \cdot L^{-1}$.

2.5. Adsorption: Kinetic Study

Adsorption kinetics have always been considered an important tool to characterize the adsorption efficiency and application prospects of an adsorbent. In this work, the adsorption kinetics were assessed at regular intervals with Cd^{2+} concentrations of 200, 300, and 400 $mg \cdot L^{-1}$; the pseudo-first-order and pseudo-second-order kinetic models are summarized as follows [33,34]:

$$q_t = q_e \times \left(1 - e^{-k_1 t}\right) \quad (3)$$

$$q_t = k_2 q_e^2 t/1 + k_2 q_e t \quad (4)$$

where q_t ($mg \cdot g^{-1}$) is the Cd^{2+} adsorption capacity at time t, t (min) is the contact time, and k_1 (min^{-1}) and k_2 ($g \cdot mg^{-1} \cdot min^{-1}$) are the rate constants of pseudo-first-order and pseudo-second-order adsorption, respectively.

Furthermore, the Weber–Morris diffusion model was also used to fit the experimental data, to evaluate the rate-limiting step during the overall adsorption process [35]. The Langmuir, Freundlich, and Redlich–Peterson isotherm models were tested, and the specific methods are referred to related studies [36,37].

2.6. Adsorption: Equilibrium Study

The adsorption isotherms on LF@AA were obtained with different Cd^{2+} concentrations from 0 to 500 mg·L^{-1} at 25, 35, and 45 °C. In this work, the Langmuir, Freundlich, and Redlich–Peterson isotherm models were tested, and the nonlinear forms are as follows:

$$q_e = \frac{q_m K_L C_e}{1 + K_L C_e} \tag{5}$$

$$q_e = K_F C_e^{1/n} \tag{6}$$

$$q_e = \frac{K_{RP} C_e}{1 + a_{RP} C_e^{\beta}} \tag{7}$$

where C_e is the equilibrium concentration of Cd^{2+} (mg·L^{-1}), q_e is the amount of Cd^{2+} adsorbed at equilibrium (mg·g^{-1}), q_m is the maximum adsorption capacity (mg·g^{-1}), and K_L (L·mg^{-1}) is the Langmuir binding constant, which is related to the energy of adsorption; K_F (mg$^{1-1/n}$·L$^{1/n}$·g^{-1}) and $1/n$ are Freundlich constants representing the adsorption capacity and adsorption intensity, respectively; K_{RP} (L·g^{-1}), a_{RP} ((L·mg^{-1})$^{\beta}$), and β ($0 < \beta < 1$) are Redlich−Peterson isotherm constants.

2.7. Regeneration

Eight cycles of regeneration and reutilization were performed to investigate the reusability of LF@AA. Typically, 20 mg of adsorbent was added to 20 mL of Cd^{2+} solution (400 mg/L), shaken (150 rpm) for 4 h, and separated by filtration. After filtration, the adsorption capacity of LF@AA was obtained by measuring the concentration of Cd^{2+} in the supernatant. Afterward, the adsorbent was washed alternately with 0.1 M HCl (desorption agent) and 0.1 M NaOH (active agent). After washing, the adsorbent continued to be reused. The regeneration study was conducted by suspending adsorbent-saturated Cd^{2+} into eluted solution with different concentrations (0.1–1.5 mol·L^{-1}) and vibrating at 25 °C for 6 h. Then, the adsorbent was separated via filtration, and the Cd^{2+} concentration was determined using the aforementioned determinate methods.

The desorption rate was calculated as follows:

$$\text{Desorption rate } (\%) = C_n V / m q_{n-1} \times 100\% \tag{8}$$

where m (g) is the adsorbent weight, q_n (mg/g) is the adsorption capacity, C_n (mg/L) is the equilibrium concentration of Cd^{2+} at cycle number n, and V (L) is the solution volume.

3. Results and Discussion

3.1. Adsorbent Characterization

After modification, the fiber of LF@AA was uniformly thickened, and after drying, it could be found that LF@AA still maintained the natural three-dimensional spongy structure of Luffa, which indicated that the ultraviolet photocatalytic grafting technology could be used to uniformly graft polyacrylic acid on the Luffa fiber skeleton. SEM/EDS analysis results of the loofah fiber samples at different stages are shown in Figure 1. Noteworthy differences were observed between the surface topography of the LF (Figure 1a) and that of LF@AA (Figure 1b). As represented in Figure 1a, the surface of LF was moderately smooth and has no discernible porous structures on it, whereas the LF@AA (Figure 1b) surface was rougher, irregular, striped, and porous, the porosity of the adsorbent was increased significantly, and the specific surface area and pore volume were increased correspondingly. The results of energy spectrum analysis showed that the composition of elements on the surface of LF had changed obviously. The proportion of C and O elements on the surface of LF was 45.96% and 54.04%, while the proportions of C and O elements became 32.62% and 34.89% after modification, and a large number of Na elements were discovered. This is because LF is mainly composed of cellulose, and its surface elements are mainly C and O. The grafting successfully introduced -COOH of polyacrylic acid. After NaOH treatment,

carboxyl groups on the surface of LF existed in the form of -COO-Na, thus affecting the element composition of the surface of LF, which also indicates that successful grafting had occurred on the surface of LF [38].

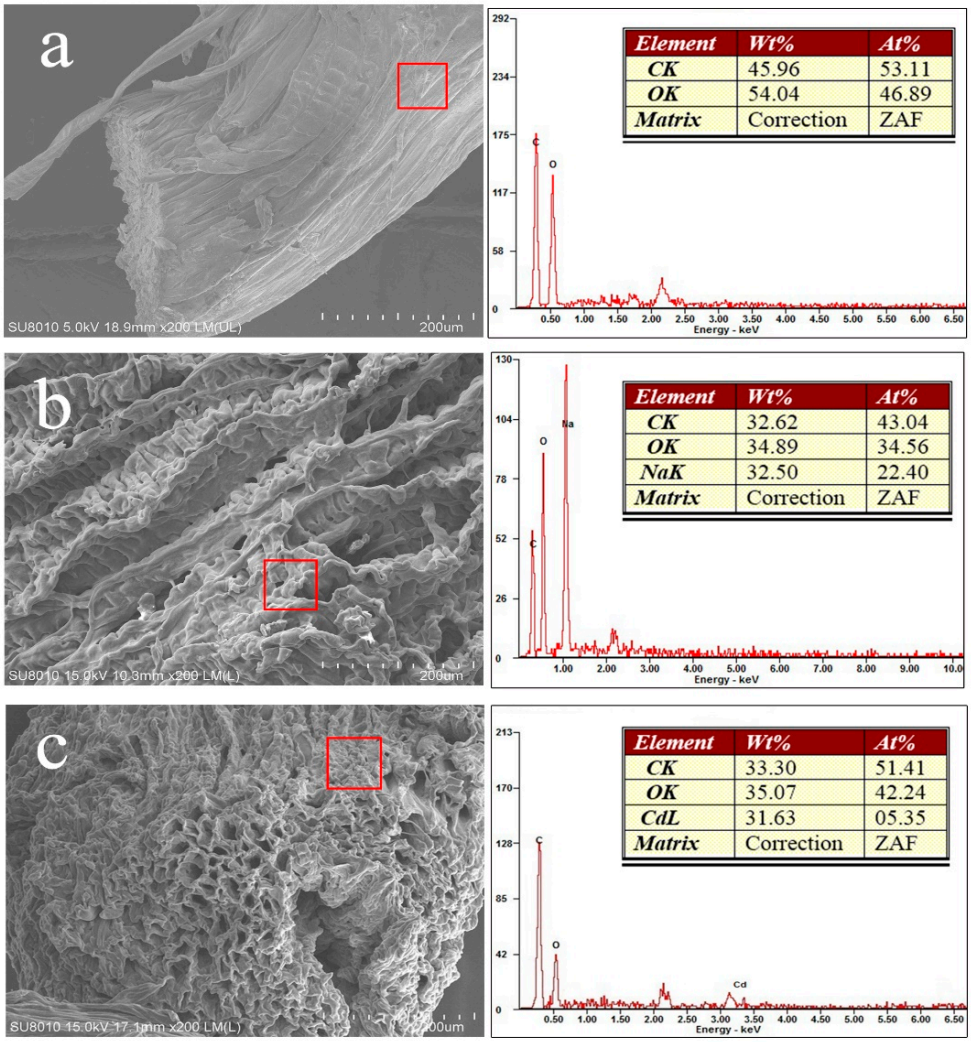

Figure 1. SEM/EDS analysis of LF (**a**), LF@AA (**b**), and Cd^{2+} adsorbed LF@AA (**c**).

It was revealed that the change in surface structure was due to the successful attachment of polymer chains to the surface [12,38,39]. Furthermore, after the adsorption was completed, EDS showed that the Cd element appeared on the surface of LF@AA (Figure 1c), with content as high as 31.63%, while Na content decreased significantly, indicating that ion exchange had occurred at the adsorption site [14]. Meanwhile, fiber bundles of LF@AA and Cd^{2+}-adsorbed LF@AA were looser than natural loofah, suggesting that UV-induced polymerization has good effects on the disaggregation of fiber bundles.

Figure 2 shows the FTIR spectrum of natural loofah samples; for LF, some absorption peaks could be identified at ca. 3337 cm^{-1} (the stretching vibration of –OH and -NH_2), ca. 2892 and 1638 cm^{-1} (the stretching vibrations of the C–H bond and carbonyl stretching of para-substituted ketones or aryl aldehydes) [40], and ca. 1162, 895, and 1018 cm^{-1} (belonged to asymmetric bridge C–O–C stretching, ß-glucoside linkage, and C–O, C–C stretching vibrations or C–OH bending in hemicelluloses, respectively) [39]. In the FTIR spectra of LF@AA, there appeared to be three new characteristic absorption peaks at 1696, 1450, and 1162 cm^{-1}, which are related to the stretching vibration of C=O, stretching vibration, and symmetrical stretching of -COO groups [41], reflecting that carboxyl groups were grafted onto the LF. After Cd^{2+} adsorbed, the C=O stretching peak of LF@AA red-

shifted about 94 cm^{-1} to 1602 cm^{-1}. With a new peak at 1317 cm^{-1}, it could be concluded that the carboxyl salt was established [42,43]. Meanwhile, the peak at 1160 cm^{-1} was no longer obvious, indicating that the adsorbed Cd^{2+} has formed a bidentate chelation with -COO- sites.

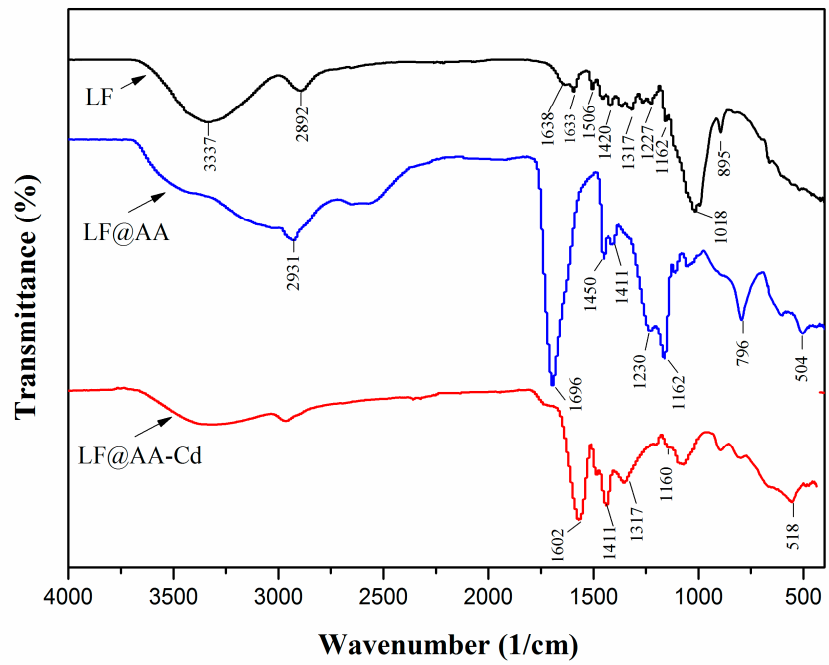

Figure 2. FTIR of LF, LF@AA, and Cd^{2+}-adsorbed LF@AA (LF@AA-Cd).

3.2. Effect of pH

The pH value of the working solution is one of the steering parameters that affect the adsorption capacity of adsorbate onto the adsorbent by influencing the degree of ionization, protonation of the functional groups of the adsorbents, adsorbent surface charge, and the types of metal [19]. Figure 3a demonstrates the effect of pH on the adsorption capacity of LF@AA and natural LF. To prevent the formation of precipitates by the combination of metal ions and hydroxyl ions, the initial pH was below 7.0. Under strongly acidic conditions (pH = 2.0), the adsorption capacity of LF and LF@AA for Cd^{2+} was at a low level, which was 24.1 mg/g and 143.7 mg/g, respectively. With the increase in pH, the adsorption capacity of LF@AA increased substantially, while that of LF did not increase significantly. In the pH range of 4–7, the adsorption capacity of LF@AA for Cd^{2+} could be kept at 315.0 mg/g, which is about 9 times that of LF. The adsorption capacity of LF@AA for Cd^{2+} was significantly increased compared with that of natural LF, indicating that the carboxyl group was effectively grafted with LF. The adsorption capacity of LF@AA was minimum at pH 2.0, which may be because there are countless positive charges (H^+) on the surface of the adsorbent under strongly acidic conditions, and H^+ has a higher concentration and mobility, which is preferentially adsorbed and competes with Cd^{2+} cations, hinders its adsorption, and thus provides a huge static repulsive force [19]. In addition, at low pH, the Coulomb repulsion also hinders the adsorption of metal ions.

The results of the Zeta potential measurement (Figure 3b) showed that the surface of LF@AA was negatively charged, the charge intensity built up over the increase in pH, and correspondingly, the adsorption capacity of positively charged Cd^{2+} was also enhanced. As expected, the adsorption capacity of LF@AA increased sharply with the increase in pH and reached a higher level at pH 4.0–7.0, indicating that the LF@AA could effectively remove Cd^{2+} from wastewater in a wide range of pH values. When the pH value is higher, the weak acidic carboxyl group is deprotonated, more negative binding sites are produced, the attraction for positively charged metal ions is correspondingly enhanced, and the

adsorption capacity is enhanced [44]. On the other hand, the adsorption of the exposed surface functional groups, porous structure, and -COO- groups from grafting may enhance the adsorption capacity of LF@AA.

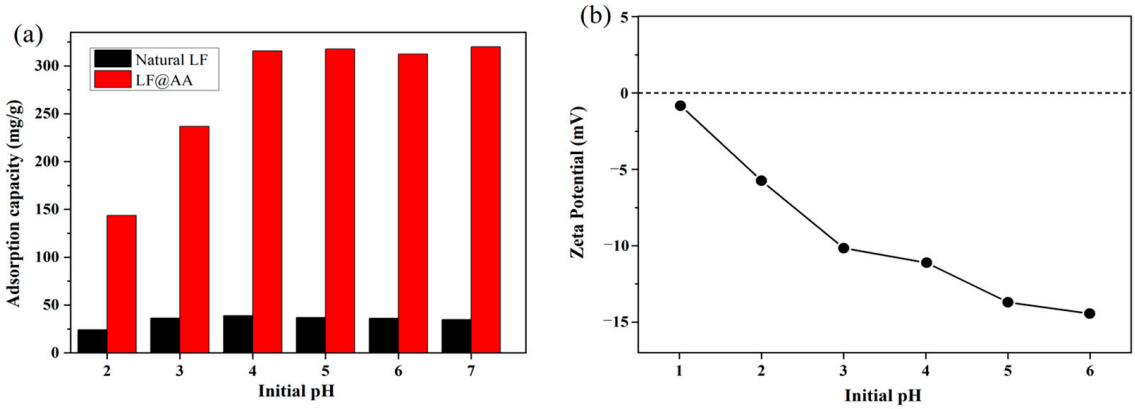

Figure 3. (**a**) Adsorption capacity at different pH values. (**b**) The Zeta potential of the adsorbent varies with pH values.

3.3. Effect of Ionic Strength

In a check to see the practical application properties of LF@AA, and offers further reveal the adsorption principle, the effects of ionic strength were studied. The result (Figure 4) showed that the adsorption efficiency of LF@AA is negatively correlated with the concentration of alkali metal ions. During the adsorption, the main adsorption mechanism should be ion exchange. Cd^{2+} was drawn to the adsorbent surface by electrostatic binding, and then, ion exchange occurred to form a bidentate chelate. When a large number of impurities in cations coexisted in an aqueous solution, there would be fierce competition between the target adsorbate and impurity cations. Moreover, as the main driving force between Cd^{2+} and LF@AA, electrostatic binding plays an important role. In the presence of Na^{+} and K^{+}, the electrostatic shielding effect should be one of the principal factors leading to the obvious decrease in the adsorption of LF@AA [12,45]. Nevertheless, it was relevant that the adsorption capacity is maintained a high level, even when the alkaline metal ion concentration is approximately 25 times the initial concentration of Cd^{2+}. This also suggests that the affinity of Cd^{2+} in the adsorption site is stronger than that of Na^{+} and K^{+} due to the higher valence, and it is preferred to form bidentate chelation with -COO- sites.

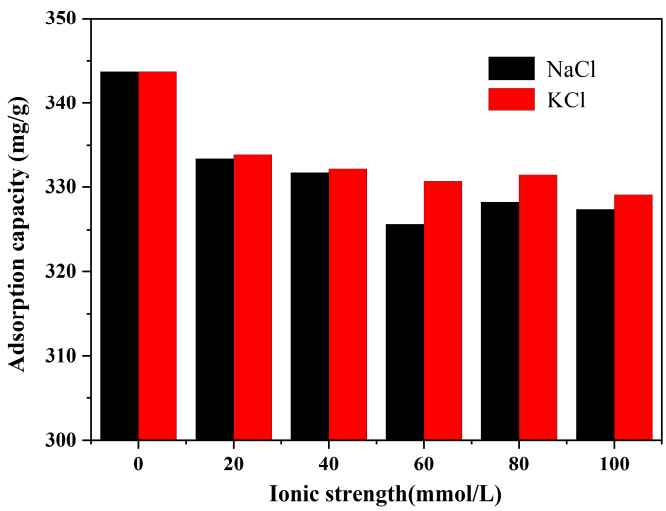

Figure 4. Adsorption capacity of Cd^{2+} by LF@AA at different ionic strengths.

3.4. Kinetic Study

The adsorption equilibrium time is one of the crucial factors affecting the mass production of an adsorbent. The effect of different reaction times (1–480 min) and different pollutant concentrations (200–400 mg·L^{-1}) on the adsorption capacity was investigated. The results (Figure 5) indicated that the adsorption capacity of Cd^{2+} increased rapidly at the beginning of the reaction, and the adsorption capacity was close to saturation at 50 min. After 50 min, the adsorption capacity increased slowly with the increase in contact time, and the adsorption reaction gradually approached equilibrium. The saturated adsorption capacity increased with the increasing initial Cd^{2+} concentration. When the initial Cd^{2+} concentration increased from 200 mg·L^{-1} to 400 mg·L^{-1}, the saturated adsorption capacity correspondingly increased from 180.8 mg·L^{-1} to 330.9 mg·L^{-1}. This suggests that the porous structure of modified LF@AA and a large number of -COO- groups produced by grafting provide convenient conditions for the adsorption of Cd^{2+}.

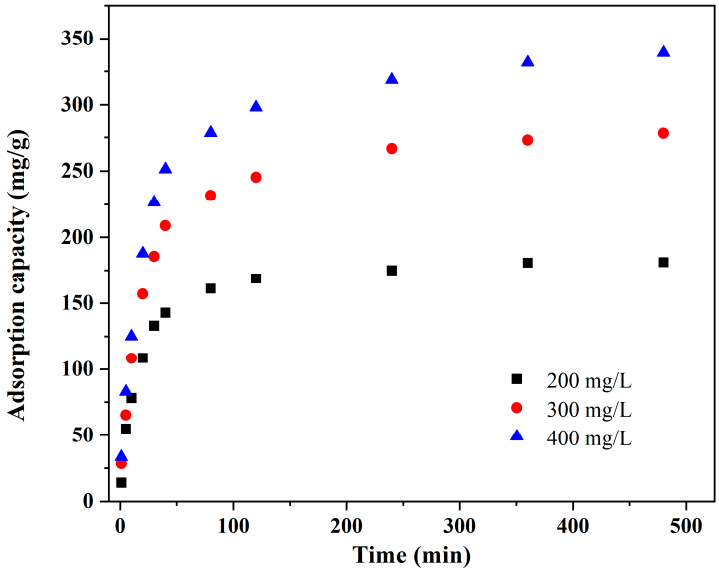

Figure 5. Effects of initial concentration and contact time on Cd^{2+} adsorption.

The change tendency of the adsorption rate may be explained by the following reasons: firstly, under the action of ion exchange and charge neutralization, Cd^{2+} quickly migrated and adsorbed to the adsorbent surface. While the adsorption capacity on the adsorbent surface was close to saturation, the metal ions diffused into the pores of LF@AA and were gradually adsorbed on the inner surface. Internal diffusion is more difficult than surface adsorption, and this adsorption process takes a longer time, and a prolonged adsorption process leads to slow growth of the adsorption capacity in the later period [46].

To further explore the adsorption mechanism of LF@AA for Cd^{2+}, the kinetic model and intraparticle diffusion model were carried out to fit the adsorption process. Table 1 and Figure 6a shows the results of the pseudo-first-order and pseudo-second-order kinetic models fitting in three different initial Cd^{2+} concentrations. The constants of these kinetic models (Table 2) show that compared with $q_{e,calc,1}$, $q_{e,calc,2}$ comes closer to the experimental value ($q_{e,exp}$). Moreover, compared with the pseudo-first-order equation, the pseudo-second-order equation had larger R^2 values (0.9974~0.9862), which suggests that the pseudo-second-order equation had a better fitting effect on the adsorption process of Cd^{2+}. To be more specific, chemisorption may be the rate-determining step in Cd^{2+} adsorption, which involves the exchange of electrons between heavy metal ions and LF@AA. In addition, the adsorption rate is in direct proportion to the square of the number of free sites, which accords with the term $(q_e - q_t)^2$ in the pseudo-second-order model [46].

Table 1. Coefficients of kinetic models.

C_0 (mg·L^{-1})	$q_{e,exp}$ (mg·g^{-1})	Pseudo-First-Order Model				Pseudo-Second-Order Model			
		k_1 (min^{-1})	$q_{e,cal,1}$ (mg·g^{-1})	R^2	SSE (%)	k_2 (g·mg^{-1}·min^{-1})	$q_{e,cal,2}$ (mg·g^{-1})	R^2	SSE (%)
200	181.2	0.05318	172.4	0.9794	8.8	0.000447	184.4	0.9974	3.2
300	279.5	0.04791	257.9	0.9733	21.6	0.000234	281.3	0.9964	1.8
400	337.0	0.04459	314.9	0.9632	22.1	0.000188	340.1	0.9862	3.1

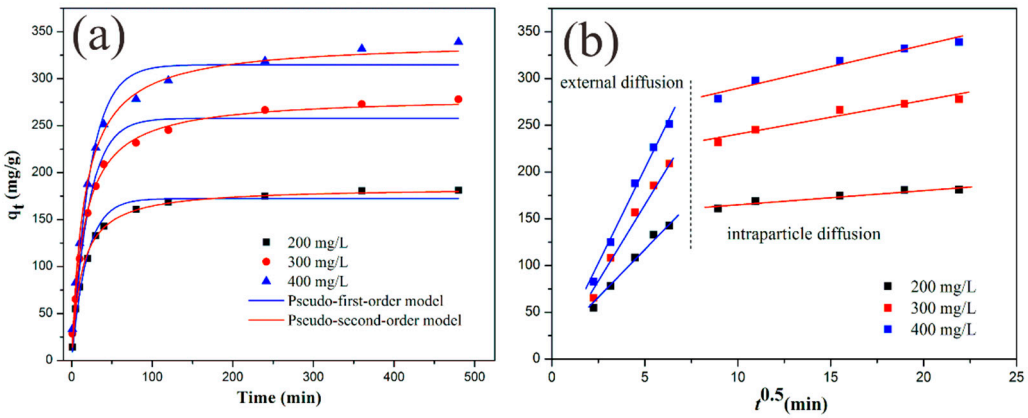

Figure 6. Fitting of kinetics models (**a**) and intraparticle diffusion model (**b**) for Cd^{2+} adsorption on LF@AA.

Table 2. Parameters of Weber–Morris model.

C_0 (mg·L^{-1})	First Stage (External Diffusion)		Second Stage (Intraparticle Diffusion)	
	$k_{i,1}$(mg·g^{-1}·min$^{-0.5}$)	R^2	$k_{i,2}$ (mg·g^{-1}·min$^{-0.5}$)	R^2
200	24.23	0.9833	150.12	0.9051
300	34.87	0.9862	205.12	0.9188
400	42.15	0.9854	244.12	0.9469

The relationship between q_t and $t^{0.5}$ of Cd^{2+} adsorption under different pollutant concentrations was studied. The results (Figure 6b) showed that despite the different initial concentrations, the q_t and $t^{0.5}$ could be fitted by a high slope straight line and a low slope straight line in turn. In the first stage, the adsorption rate was fast, and the adsorption capacity reached about 75% of the equilibrium adsorption capacity in the first 40 min, which was due to the rapid binding of adsorption sites on the adsorbent surface with Cd^{2+} in this stage. With the progress of adsorption, a large number of sites on the surface of the adsorbent were occupied. To achieve further adsorption, Cd^{2+} needs to diffuse into the pores of the adsorbent to complete the adsorption. Therefore, the rate control step in the second stage is mainly the internal diffusion process, and the adsorption rate becomes slower. The relevant parameters of the Weber–Morris model are contained in Table 2. It can be seen that R^2 was greater than 0.9 under different initial pollutant concentrations, indicating that the Weber–Morris model is suitable for fitting the adsorption process of LF@AA. Furthermore, inner diffusion is more time-consuming than outer diffusion [47]. Therefore, the results of the kinetic analysis showed that both external and internal diffusion played a part in the process of cadmium adsorption by LF@AA, and the internal diffusion should be dominant.

3.5. Adsorption Isotherms

The effect of temperature on the adsorption properties of LF@AA was analyzed. The results (Figure 7) showed that the saturated adsorption capacity was positively correlated with temperature. When the temperature increased from 303.15 K to 313.15 K and 323.15 K,

the saturated adsorption capacity increased from 345.0 mg·g^{-1} to 347.7 and 352.8 mg·g^{-1}, respectively. The adsorption capacity was increased with the increase in temperature, but the effect was not significant. Generally speaking, the activity of metal ions and adsorbents increased with the increase in temperature, and the interaction between solvent and solid surface decreased with the increase in temperature. Therefore, the higher the temperature, the easier the transfer and diffusion of adsorbates to the adsorbent surface and the more adsorption sites are exposed, which enhances the possibility of adsorbent adsorption.

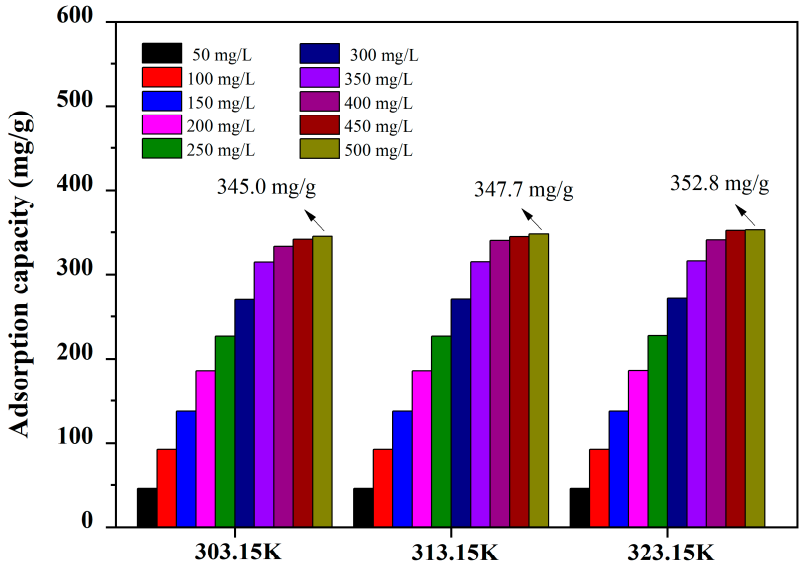

Figure 7. Adsorption capacity at different temperatures.

Redlich–Peterson, Langmuir, and Freundlich models were utilized to fit the isotherm adsorption curve of Cd^{2+}. The fitted-curve and model parameters are shown in Figure 8 and Table 3, respectively. The results showed that the average R^2 values of the Redlich–Peterson and Langmuir models were greater than 0.97, indicating a significant correlation. In addition, the error between the calculated values of q_m of Langmuir fitted-curve and the experimental results was less than 3%, indicating that the adsorption characteristic of LF@AA is consistent with monolayer adsorption. The Redlich–Peterson isotherm has the has the characteristics of both Langmuir and Freundlich isotherms [37]. The β values of Redlich–Peterson and Langmuir isotherms converged with the increase in temperature, which may be due to the uniform distribution of binding sites on the surface of the adsorption medium.

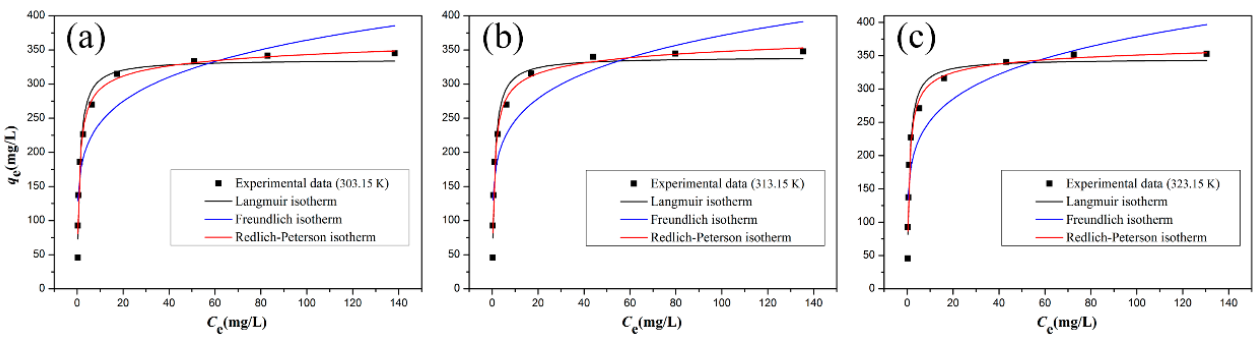

Figure 8. Non-linear fitting curves of isotherms for 303.15K (**a**), 313.15K (**b**) and 323.15K (**c**).

Table 3. Parameters of the adsorption isotherm.

T (K)	Langmuir Isotherm Constants			Freundlich Isotherm Constants			Redlich−Peterson Isotherm Constants			
	q_m (mg·g^{-1})	K_L (L·mg^{-1})	R^2	K_F (mg$^{1-1/n}$·L$^{1/n}$·g^{-1})	*1/n*	R^2	K_{RP}(m·mg^{-1})	α_{RP} (L$^{\beta}$·mg$^{-\beta}$)	β	R^2
25 °C	335.9	1.0201	0.9706	162.28	0.1756	0.8339	421.57	1.4757	0.9584	0.9768
35 °C	339.6	1.0278	0.9699	163.80	0.1776	0.8309	427.22	1.4781	0.9581	0.9760
45 °C	345.2	1.1386	0.9723	168.22	0.1761	0.8231	447.53	1.4540	0.9698	0.9736

3.6. Regeneration

Reusability is an important consideration in determining whether a new adsorbent can be used in practice. The reusability of LF@AA was verified based on eight consecutive adsorption cycles. The result (Figure 9) shows that the total adsorption capacity of LF@AA for Cd^{2+} decreased slightly from 339.3 to 318.8 mg/g after eight consecutive cycles, only decreasing by 6.0%, indicating that LF@AA had a stable adsorption efficiency in the reuse process. Compared with the reported results, the reusability of LF@AA is also quite satisfactory [21,48]. Therefore, LF@AA has a large adsorption capacity and can be reused many times, which has the potential to become a cost-effective heavy metal adsorbent.

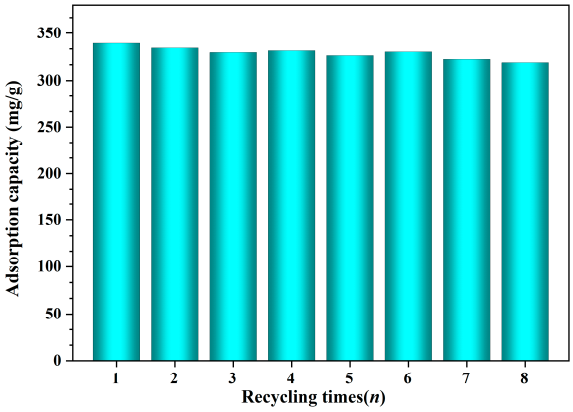

Figure 9. Effect of recycling times on adsorption capacity.

4. Conclusions

In this work, a novel three-dimensional natural polymer network-based adsorbent was successfully prepared via UV-induced polymerization, allowing a uniform polymer brush on the matrix to be obtained, which resulted in an outstanding adsorption capacity of 339.3 mg·g^{-1} and widely applicative pH range (4.0–7.0) for the removal of Cd^{2+}. Moreover, the coexistence of cations (Na^+ and K^+) in solutions is unfavorable to the adsorption of Cd^{2+}, and the order is $Na^+ > K^+$. According to the characterization analysis, the main adsorption mechanism should be ion exchange. The Cd^{2+} electrostatically adsorbed on the surface of the adsorbent was synthesized into a bidentate chelate under the action of ion exchange. The results of the adsorption kinetics analysis showed that the adsorption process of Cd^{2+} was divided into external diffusion and internal diffusion and followed the pseudo-second-order kinetic and the Weber–Morris equations. The adsorption isotherm parameters showed that the adsorption process followed the Langmuir and Redlich–Peterson models. In addition, the excellent reusability of LF@AA was also confirmed after eight-time regeneration. The excellent adsorption performance of LF@AA makes it an attractive adsorbent for the treatment of water contaminated with Cd^{2+} and realizes the high added-value utilization of natural cellulose.

Author Contributions: Conceptualization, H.X.; Data curation, J.W.; Formal analysis, H.X. and M.X.; Funding acquisition, F.M.; Investigation, H.X.; Methodology, H.X.; Project administration, F.M.; Resources, C.L.; Software, M.X.; Supervision, F.M.; Validation, Y.Y.; Visualization, H.X. and C.L.; Writing—original draft, H.X.; Writing—review & editing, C.L. and F.M. All authors will be informed

about each step of manuscript processing including submission, revision, revision reminder, etc., via emails from our system or assigned Assistant Editor. All authors have read and agreed to the published version of the manuscript.

Funding: This research was funded by Joint Research Project II on Ecological Environment Protection and Restoration of the Yangtze River, grant number (2022-LHYJ-02-0506-09).

Data Availability Statement: The data presented in this study are available on request from the corresponding author.

Conflicts of Interest: The authors declare no conflict of interest.

References

1. Åkesson, A.; Barregard, L.; Bergdahl, I.A.; Nordberg, G.F.; Nordberg, M.; Skerfving, S. Non-Renal effects and the risk assessment of environmental cadmium exposure. *Environ. Health Perspect.* **2014**, *122*, 431–438. [CrossRef]
2. Marques, P.; Rosa, M.F.; Pinheiro, H.M. pH effects on the removal of CU^{2+}, Cd^{2+} and Pb^{2+} from aqueous solution by waste brewery biomass. *Bioprocess Eng.* **2000**, *23*, 135–141. [CrossRef]
3. EL-Hendawy, A.A. The role of surface chemistry and solution pH on the removal of Pb^{2+} and Cd^{2+} ions via effective adsorbents from low-cost biomass. *J. Hazard. Mater.* **2009**, *167*, 260–267. [CrossRef]
4. Yang, G.; Wang, Z.; Xian, Q.; Shen, F.; Sun, C.; Zhang, Y.; Wu, J. Effects of pyrolysis temperature on the physicochemical properties of biochar derived from vermicompost and its potential use as an environmental amendment. *Rsc Adv.* **2015**, *5*, 40117–40125. [CrossRef]
5. Wan Ngah, W.S.; Hanafiah, M.A.K.M. Removal of heavy metal ions from wastewater by chemically modified plant wastes as adsorbents: A review. *Bioresour. Technol.* **2008**, *99*, 3935–3948. [CrossRef]
6. Feng, N.; Guo, X.; Liang, S.; Zhu, Y.; Liu, J. Biosorption of heavy metals from aqueous solutions by chemically modified orange peel. *J. Hazard. Mater.* **2011**, *185*, 49–54. [CrossRef]
7. Shakya, A.; Agarwal, T. Removal of Cr(VI) from water using pineapple peel derived biochars: Adsorption potential and re-usability assessment. *J. Mol. Liq.* **2019**, *293*, 111497. [CrossRef]
8. Lemraski, E.G.; Sharafinia, S. Kinetics, equilibrium and thermodynamics studies of Pb^{2+} adsorption onto new activated carbon prepared from Persian mesquite grain. *J. Mol. Liq.* **2016**, *219*, 482–492. [CrossRef]
9. Mayakaduwa, S.S.; Kumarathilaka, P.; Herath, I.; Ahmad, M.; Al-Wabel, M.; Ok, Y.S.; Usman, A.; Abduljabbar, A.; Vithanage, M. Equilibrium and kinetic mechanisms of woody biochar on aqueous glyphosate removal. *Chemosphere* **2016**, *144*, 2516–2521. [CrossRef]
10. Xu, X.; Gao, B.; Huang, X.; Ling, J.; Song, W.; Yue, Q. Physicochemical characteristics of epichlorohydrin, pyridine and trimethylamine functionalized cotton stalk and its adsorption/desorption properties for perchlorate. *J. Colloid Interface Sci.* **2015**, *440*, 219–228. [CrossRef]
11. Hokkanen, S.; Bhatnagar, A.; Sillanpaa, M. A review on modification methods to cellulose-based adsorbents to improve adsorption capacity. *Water Res.* **2016**, *91*, 156–173. [CrossRef]
12. Zhou, Q.; Yang, H.; Yan, C.; Luo, W.; Li, X.; Zhao, J. Synthesis of carboxylic acid functionalized diatomite with a micro-villous surface via UV-induced graft polymerization and its adsorption properties for Lanthanum(III) ions. *Colloids Surf. A* **2016**, *501*, 9–16. [CrossRef]
13. Li, X.J.; Yan, C.J.; Luo, W.J.; Gao, Q.; Zhou, Q.; Liu, C.; Zhou, S. Exceptional cerium(III) adsorption performance of poly(acrylic acid) brushes-decorated attapulgite with abundant and highly accessible binding sites. *Chem. Eng. J.* **2015**, *284*, 333–342. [CrossRef]
14. Zhou, Q.; Yan, C.; Luo, W. Preparation of a novel carboxylate-rich wheat straw through surface graft modification for efficient separation of Ce(III) from wastewater. *Mater. Des.* **2016**, *97*, 195–203. [CrossRef]
15. Liu, C.; Yan, C.; Luo, W.; Li, X.; Ge, W.; Zhou, S. Simple preparation and enhanced adsorption properties of loofah fiber adsorbent by ultraviolet radiation graft. *Mater. Lett.* **2015**, *157*, 303–306. [CrossRef]
16. Chen, Q.; Shi, Q.; Gorb, S.N.; Li, Z. A multiscale study on the structural and mechanical properties of the luffa sponge from Luffa cylindrica plant. *J. Biomech.* **2014**, *47*, 1332–1339. [CrossRef]
17. Demir, H.; Atikler, U.; Balköse, D.; Tıhmınlıoğlu, F. The effect of fiber surface treatments on the tensile and water sorption properties of polypropylene–luffa fiber composites. *Compos. Part A Appl. Sci. Manuf.* **2006**, *37*, 447–456. [CrossRef]
18. Thakur, V.K.; Thakur, M.K. Processing and characterization of natural cellulose fibers/thermoset polymer composites. *Carbohydr. Polym.* **2014**, *109*, 102–117. [CrossRef]
19. Alhijazi, M.; Safaei, B.; Zeeshan, Q.; Asmael, M.; Qin, Z. Recent Developments in Luffa Natural Fiber Composites: Review. *Sustainability* **2020**, *12*, 7683. [CrossRef]
20. Khadir, A.; Motamedi, M.; Pakzad, E.; Sillanpää, M.; Mahajan, S. The prospective utilization of Luffa fibres as a lignocellulosic bio-material for environmental remediation of aqueous media: A review. *J. Environ. Chem. Eng.* **2020**, *9*, 104691. [CrossRef]
21. Shahidi, A.; Jalilnejad, N.; Jalilnejad, E. A study on adsorption of cadmium(II) ions from aqueous solution using Luffa cylindrica. *Desalination Water Treat.* **2015**, *53*, 3570–3579. [CrossRef]

22. Ahmad, R.; Haseeb, S. Kinetic, isotherm and thermodynamic studies for the removal of Pb^{2+} ion by a novel adsorbent Luffa acutangula (LAPR). *Desalination Water Treat.* **2015**, *57*, 17826–17835. [CrossRef]
23. Zhang, J.; Yang, J.; Tian, Q.; Liang, X.; Zhu, Y.; Sand, W.; Li, F.; Ma, C.; Liu, Y.; Yang, B. Durability and performance of loofah sponge as carrier for wastewater treatment with high ammonium. *Water Environ. Res.* **2019**, *91*, 581–587. [CrossRef]
24. Tang, X.; Zhang, Q.; Liu, Z.; Pan, K.; Dong, Y.; Li, Y. Removal of Cu(II) by loofah fibers as a natural and low-cost adsorbent from aqueous solutions. *J. Mol. Liq.* **2014**, *191*, 73–78. [CrossRef]
25. Liu, C.; Yan, C.; Zhou, S.; Ge, W. Fabrication of sponge biomass adsorbent through UV-induced surface-initiated polymerization for the adsorption of Ce(III) from wastewater. *Water Sci. Technol.* **2017**, *75*, 2755–2764. [CrossRef]
26. Ahmadi, M.; Vahabzadeh, F.; Bonakdarpour, B.; Mehranian, M.; Mofarrah, E. Phenolic removal in olive oil mill wastewater using loofah-immobilized Phanerochaete chrysosporium. *World J. Microbiol. Biotechnol.* **2006**, *22*, 119–127. [CrossRef]
27. Sriharsha, D.V.; Lokesh; Kumar, R.; Savitha, J. Immobilized fungi on Luffa cylindrica: An effective biosorbent for the removal of lead. *J. Taiwan Inst. Chem. Eng.* **2017**, *80*, 589–595.
28. Oun, A.A.; Kamal, K.H.; Farroh, K.; Ali, E.F.; Hassan, M.A. Development of fast and high-efficiency sponge-gourd fibers (Luffa cylindrica)/hydroxyapatite composites for removal of lead and methylene blue. *Arabian J. Chem.* **2021**, *14*, 103281. [CrossRef]
29. Li, S.; Liu, F.; Su, Y.; Shao, N.; Zhang, Z. Luffa sponge-derived hierarchical meso/macroporous boron nitride fibers as superior sorbents for heavy metal sequestration. *J. Hazard. Mater.* **2019**, *378*, 120669. [CrossRef]
30. Khadir, A.; Negarestani, M.; Mollahosseini, A. Sequestration of a non-steroidal anti-inflammatory drug from aquatic media by lignocellulosic material (Luffa cylindrica) reinforced with polypyrrole: Study of parameters, kinetics, and equilibrium. *J. Environ. Chem. Eng.* **2020**, *8*, 103734. [CrossRef]
31. Shih, Y.J.; Dong, C.D.; Huang, Y.H.; Huang, C.P. Electro-sorption of ammonium ion onto nickel foam supported highly microporous activated carbon prepared from agricultural residues (dried Luffa cylindrica). *Sci. Total Environ.* **2019**, *673*, 296–305. [CrossRef]
32. Xiao, F.; Cheng, J.; Cao, W.; Yang, C.; Chen, J.; Luo, Z. Removal of heavy metals from aqueous solution using chitosan-combined magnetic biochars. *J. Colloid Interface Sci.* **2019**, *540*, 579–584. [CrossRef]
33. Azizian, S. Kinetic models of sorption: A theoretical analysis. *J. Colloid Interface Sci.* **2004**, *276*, 47–52. [CrossRef]
34. Ghaedi, M.; Hassanzadeh, A.; Kokhdan, S.N. Multiwalled carbon nanotubes as adsorbents for the kinetic and equilibrium study of the removal of alizarin red s and morin. *J. Chem. Eng. Data* **2011**, *56*, 2511–2520. [CrossRef]
35. Ho, Y.S.; Mckay, G. Sorption of dye from aqueous solution by peat. *Chem. Eng. J.* **1998**, *70*, 115–124. [CrossRef]
36. Tan, I.A.; Hameed, B.H.; Ahmad, A.L. Equilibrium and Kinetic Studies on Basic Dye Adsorption by Oil Palm Fibre Activated Carbon. *Chem. Eng. J.* **2007**, *127*, 111–119. [CrossRef]
37. Redlich, O.; Peterson, D.L. A useful adsorption isotherm. *J. Phys. Chem.* **2007**, *63*, 1024. [CrossRef]
38. Karlsson, J.O.; Henriksson, Å.; Michálek, J.; Gatenholm, P. Control of cellulose-supported hydrogel microstructures by three-dimensional graft polymerization of glycol methacrylates. *Polymer* **2000**, *41*, 1551–1559. [CrossRef]
39. Gupta, V.K.; Agarwal, S.; Singh, P.; Pathania, D. Acrylic acid grafted cellulosic Luffa cylindrical fiber for the removal of dye and metal ions. *Carbohydr. Polym.* **2013**, *98*, 1214–1221. [CrossRef]
40. Tarley, C.R.T.; Arruda, M.A.Z. Biosorption of heavy metals using rice milling by-products. Characterisation and application for removal of metals from aqueous effluents. *Chemosphere* **2004**, *54*, 987–995. [CrossRef]
41. Wang, X.; Zheng, Y.; Wang, A. Fast removal of copper ions from aqueous solution by chitosan- g -poly(acrylic acid)/attapulgite composites. *J. Hazard. Mater.* **2009**, *168*, 970–977. [CrossRef]
42. Zhang, W.M.; Jiang, Y.Q.; Cao, X.Y.; Chen, M.; Ge, D.L.; Sun, Z.X. Synthesis of pore-variable mesoporous CdS and evaluation of its photocatalytic activity in degrading methylene blue. *Mater. Res. Bull.* **2013**, *48*, 4379–4384. [CrossRef]
43. Zhao, Y.; Liu, H.; Wang, F.; Liu, J.; Chul Park, K.; Endo, M. A simple route to synthesize carbon-nanotube/cadmium-sulfide hybrid heterostructures and their optical properties. *J. Solid State Chem.* **2009**, *182*, 875–880. [CrossRef]
44. Badruddoza, A.Z.M.; Tay, A.S.H.; Tan, P.Y.; Hidajat, K.; Uddin, M.S. Carboxymethyl-β-cyclodextrin conjugated magnetic nanoparticles as nano-adsorbents for removal of copper ions: Synthesis and adsorption studies. *J. Hazard. Mater.* **2011**, *185*, 1177–1186. [CrossRef]
45. Lu, D.; Cao, Q.; Li, X.; Cao, X.; Luo, F.; Shao, W. Kinetics and equilibrium of Cu(II) adsorption onto chemically modified orange peel cellulose biosorbents. *Hydrometallurgy* **2009**, *95*, 145–152. [CrossRef]
46. Wang, S.; Zhai, Y.Y.; Gao, Q.; Luo, W.J.; Xia, H.; Zhou, C.G. Highly efficient removal of acid red 18 from aqueous solution by magnetically retrievable chitosan/carbon nanotube: Batch study, isotherms, kinetics, and thermodynamics. *J. Chem. Eng. Data* **2014**, *59*, 39–51. [CrossRef]
47. Gulipalli, C.S.; Prasad, B.; Wasewar, K.L. Batch study, equilibirum and kinetics of adsorption of selenium using rice husk ash (RHA). *J. Eng. Sci. Technol.* **2011**, *6*, 590–609.
48. Luo, S.; Li, X.; Chen, L.; Chen, J.; Wan, Y.; Liu, C. Layer-by-layer strategy for adsorption capacity fattening of endophytic bacterial biomass for highly effective removal of heavy metals. *Chem. Eng. J.* **2014**, *239*, 312–321. [CrossRef]